CHEMISTRY
A EUROPEAN JOURNAL

DOI: 10.1002/chem.200700806

Integrated, Electrically Contacted NAD(P)$^+$-Dependent Enzyme–Carbon Nanotube Electrodes for Biosensors and Biofuel Cell Applications

Yi-Ming Yan, Omer Yehezkeli, and Itamar Willner*[a]

Abstract: Integrated, electrically contacted β-nicotinamide adenine dinucleotide- (NAD^+) or β-nicotinamide adenine dinucleotide phosphate- ($NADP^+$) dependent enzyme electrodes were prepared on single-walled carbon nanotube (SWCNT) supports. The SWCNTs were functionalized with Nile Blue (**1**), and the cofactors $NADP^+$ and NAD^+ were linked to **1** through a phenyl boronic acid ligand. The affinity complexes of glucose dehydrogenase (GDH) with the $NADP^+$ cofactor or alcohol dehydrogenase (AlcDH) with the NAD^+ cofactor were crosslinked with glutaric dialdehyde and the biomolecule-functionalized SWCNT materials were deposited on glassy carbon electrodes. The integrated enzyme electrodes revealed bioelectrocatalytic activities, and they acted as amperometric electrodes for the analysis of glucose or ethanol. The bioelectrocatalytic response of the systems originated from the biocatalyzed oxidation of the respective substrates by the enzyme with the concomitant generation of NAD(P)H cofactors. The electrocatalytically mediated oxidation of NAD(P)H by **1** led to amperometric responses in the system. Similarly, an electrically contacted bilirubin oxidase (BOD)–SWCNT electrode was prepared by the deposition of BOD onto the SWCNTs and the subsequent crosslinking of the BOD units using glutaric dialdehyde. The BOD–SWCNT electrode revealed bioelectrocatalytic functions for the reduction of O_2 to H_2O. The different electrically contacted SWCNT-based enzyme electrodes were used to construct biofuel cell elements. The electrically contacted GDH–SWCNT electrode was used as the anode for the oxidation of the glucose fuel in conjunction with the BOD–SWCNT electrode in the presence of O_2, which acted as an oxidizer in the system. The power output of the cell was 23 $\mu W\,cm^{-2}$. Similarly, the AlcDH–SWCNT electrode was used as the anode for the oxidation of ethanol, which was acting as the fuel, with the BOD–SWCNT electrode as the cathode for the reduction of O_2. The power output of the system was 48 $\mu W\,cm^{-2}$.

Keywords: biofuel cells · biosensors · catalysis · cofactors · nanotubes

Introduction

Creating an electrical contact between redox enzymes and electrodes is the most fundamental principle for developing amperometric biosensors and biofuel cells.[1,2] Different methods to assemble integrated, electrically contacted enzyme electrodes have been reported, which include tethering redox mediator units to the enzymes[3] or the incorporation of the enzyme into the redox-active polymers of conducting polymers.[4] The reconstitution of enzymes onto monolayer-functionalized electrodes was used as a general paradigm for the structural alignment of the enzymes on electrode surfaces,[5] and molecular relays,[6] redox polymers,[7] metal nanoparticles,[8] and carbon nanotubes[9] were used as electrical bridges that communicate with the redox enzymes and the electrodes. The different electrically contacted biocatalytic electrodes were used as amperometric sensors for the enzyme substrates. One further application of these electrodes includes the assembly of biofuel cells.[10] The biofuel cell consists of two enzyme-modified electrodes where the anode biocatalyzes the oxidation of the fuel and the cathode biocatalyzes the reduction of the oxidizer. The concomitant oxidation and reduction processes at the electrodes yield electrical power. Most of the biofuel cells reported use glucose as the fuel and O_2 as the oxidizer, although other substrates and oxidizers, for example, H_2O_2, may be employed.[11] Indeed, the primary report on the construction of a biofuel cell based on monolayer-functionalized electrodes[12] attracted substantial research efforts, and dif-

[a] Dr. Y.-M. Yan, O. Yehezkeli, Prof. I. Willner
Institute of Chemistry
The Hebrew University of Jerusalem
Jerusalem 91904 (Israel)
Fax: (+972) 2-652-7715
E-mail: willnea@vms.huji.ac.il

ferent studies addressed the assembly of electrically contacted enzyme electrodes for enhanced electrical power output[13] and the design of biofuel cells of higher complexity, such as electroswitchable biofuel cells,[14] magnetic field controlled biofuel cells,[15] and the construction of miniaturized biofuel cells.[16]

Among the different redox enzymes that can be used as biomaterials for electrochemical biosensors or biofuel cells, β-nicotinamide adenine dinucleotide (NAD^+) or β-nicotinamide adenine dinucleotide phosphate ($NADP^+$) cofactor-dependent enzymes are of special interest. However, the incorporation of $NAD(P)^+$-dependent enzymes in such bioelectronic devices requires the development of artificial electrocatalysts for the regeneration of the $NAD(P)^+$ cofactors,[17] and the structural organization of the $NAD(P)^+$ cofactors, electrocatalysts, and the respective enzymes as integrated, nondiffusional matrices on the electrodes. Several integrated electrocatalyst–cofactor–enzyme systems were developed by the formation of affinity complexes between relay-$NAD(P)^+$ cofactor units and the respective enzymes followed by their crosslinking to yield integrated nonseparable matrices.[18] Herein, we wish to report the assembly of integrated, electrically contacted $NAD(P)^+$-dependent enzyme electrodes on single-walled carbon nanotubes (SWCNTs) that provide a conducting support with a large surface area. In contrast to previous studies that demonstrated the use of a redox-active polymer film on SWCNTs, which acts as an electrical mediator, to activate the oxidation of diffusional NADH,[19] the present study reveals methods to tailor covalently linked cofactor–enzyme architectures in a rigid nonseparable configuration on SWCNTs for biosensing and biofuel cell applications.

Results and Discussion

Different redox-active organic dyes are known to act as electrocatalysts for the oxidation of NAD(P)H and the regeneration of the $NAD(P)^+$ cofactors.[20] This function of aromatic dyes, together with the fact that polycyclic aromatic compounds strongly bind to SWCNTs through π–π interactions, suggested that redox-active aromatic dyes could be coupled to SWCNTs as mediators to provide an electrical contact for $NAD(P)^+$-dependent enzymes with electrodes. The method to tailor the integrated, electrically contacted enzyme electrode for $NAD(P)^+$-dependent biocatalysts attached to SWCNT electrodes is depicted in Scheme 1, which uses glucose dehydrogenase (GDH) and alcohol dehydrogenase (AlcDH) as model systems.

Nile Blue (**1**) was adsorbed onto SWCNTs and the resulting functionalized SWCNTs were deposited onto a glassy carbon (GC) electrode. The adsorbed dye showed a quasi-reversible redox wave, $E^{\circ\prime} = -0.35$ V versus Ag/AgCl (Figure 1A). Coulometric analysis of the redox wave of **1** indicated a surface coverage of 1.98×10^{-8} mol mg^{-1} on the SWCNTs. The ligand, 4-carboxyphenyl boronic acid (**2**), was then covalently linked to **1**. Figure 1B depicts the cyclic voltammogram of **1**/**2** associated with the SWCNTs. Two quasi-reversible waves are observed at −0.35 and −0.15 V versus Ag/AgCl. Whereas the first wave is attributed to unmodified **1** linked to the SWCNTs, the positively shifted wave is attributed to **1** linked to **2** through an amide bond. The transformation of the amine group to a more electron-accepting amide group results in the positive shift in potential. Coulometric analysis of the two waves indicates that approximately 18% of **1** was modified by **2**. The $NADP^+$ cofactor was then linked to the SWCNTs by linking the sugar units of $NADP^+$ to **2**. Subsequently, the $NADP^+$-dependent enzyme GDH was treated with the **2**–$NADP^+$ complex to form an affinity complex. Crosslinking the protein units associated with the $NADP^+$ groups by glutaric dialdehyde resulted in the rigid integrated protein coating on the SWCNTs (Scheme 1A). Similarly, the NAD^+ cofactor was linked to **2** to form the respective ribose–**2** complexes. (Note that NAD^+ has two possible binding modes, and these different association patterns and the corresponding biocatalytic activities will be discussed later.) Formation of the affinity complexes between the NAD^+ cofactor units and AlcDH followed by their crosslinking with glutaric dialdehyde generated the integrated, electrically contacted rigid enzyme electrode (Scheme 1B). It should be noted that the affinity complexes between the $NAD(P)^+$ units and the integrated proteins are labile in nature. That is, crosslinking the proteins fixes the biocatalysts onto the electrode supports, but the associated $NAD(P)^+$ cofactors freely dissociate and associate from and to the protein matrices, respectively. This dynamic movement of $NAD(P)^+$ in the porous protein structures allows the effective electrical communication between the redox enzyme and the electrode by the $NAD(P)^+$–**1** pair. Furthermore, the dynamic equilibrium binding of the $NAD(P)^+$ units enables the application of the integration paradigm on any $NAD(P)^+$-dependent enzyme, independent of the specific binding sequence of the cofactor or substrate.

Figure 2A shows the electrocatalytic anodic currents generated by the GDH-crosslinked enzyme electrode in the presence of different concentrations of glucose. As the concentration of glucose increases, the electrocatalytic anodic current is enhanced. The resulting calibration curve is shown in Figure 2B. The onset electrocatalyzed oxidation of glucose occurs at $E = -0.15$ V versus Ag/AgCl, which corresponds to the redox potential of **1** functionalized with **2** at pH 7.0. This result suggests that the units of **1** that are linked to **2**, on which GDH was reconstituted, rather than free **1**, act as the mediator units for activation of the bioelectrocatalytic functions of the enzyme. In a series of control experiments, the requirement for all three components, **1**, $NADP^+$, and GDH, to accomplish the bioelectrocatalyzed oxidation of glucose was confirmed. In one experiment, the electrode modified with the $NADP^+$–**1** conjugate was treated with diffusional GDH in the presence of glucose. The bioelectrocatalyzed oxidation of glucose was observed in this system, as expected, in agreement with the results observed for the integrated, electrically contacted electrode.

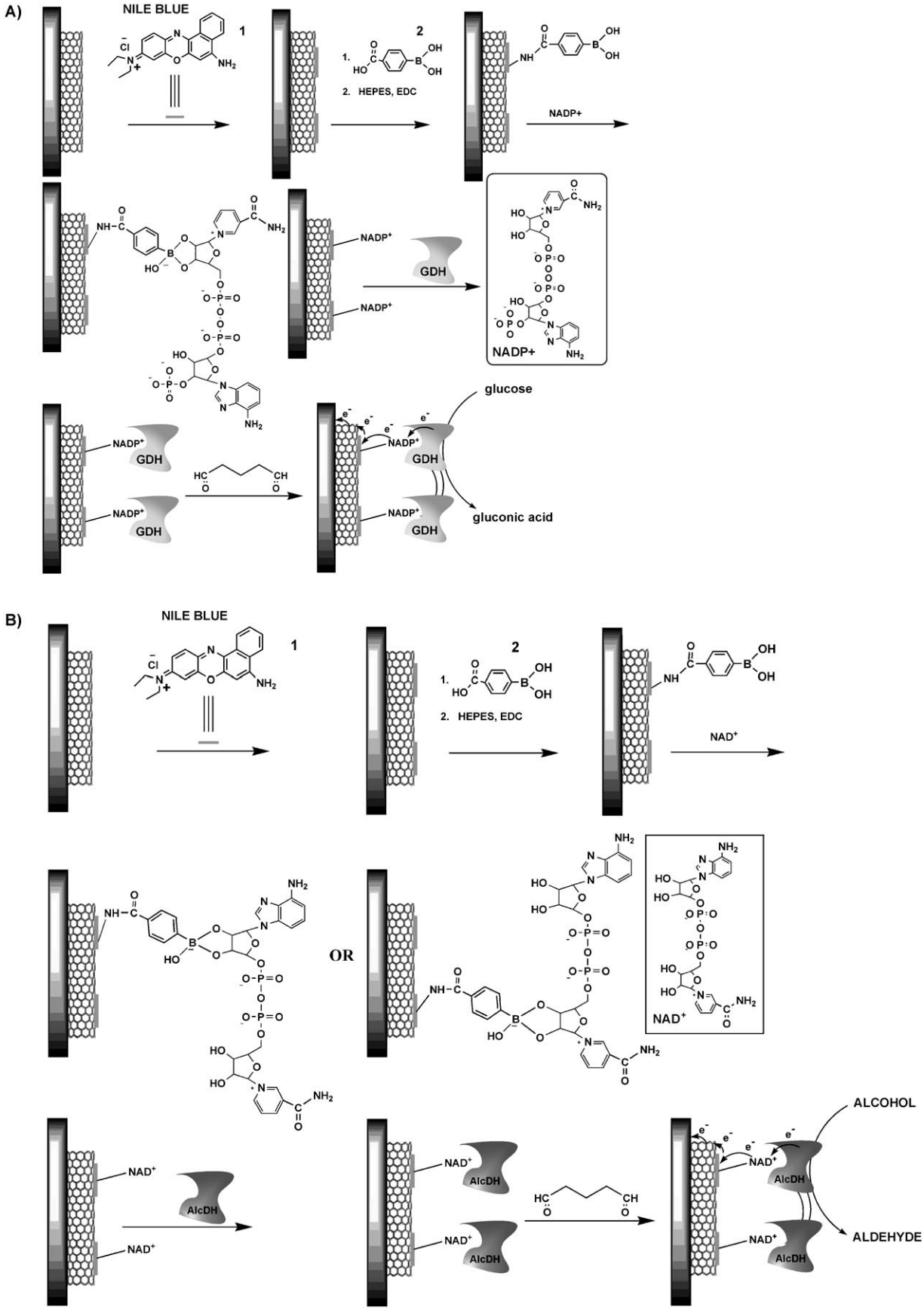

Scheme 1. A) Assembly of the integrated, electrically contacted GDH–$NADP^+$–**1**–SWCNT electrode. B) Assembly of the integrated, electrically contacted AlcDH–NAD^+–**1**–SWCNT electrode. HEPES: 4-(2-hydroxyethyl)piperazine-1-ethanesulfonic acid sodium salt, EDC: 1-ethyl-3-(3-dimethylaminopropyl)carbodiimide.

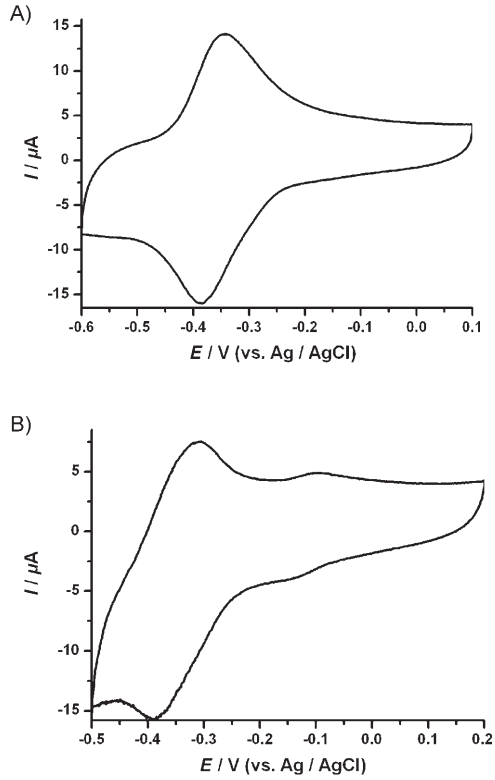

Figure 1. A) Cyclic voltammogram that corresponds to **1** adsorbed onto a SWCNT-modified GC electrode. B) Cyclic voltammogram that corresponds to **2**–**1**–SWCNT-modified GC electrode. Data recorded in 0.10 M phosphate buffer (pH 7.0) at room temperature with a potential scan rate of 100 mV s^{-1}.

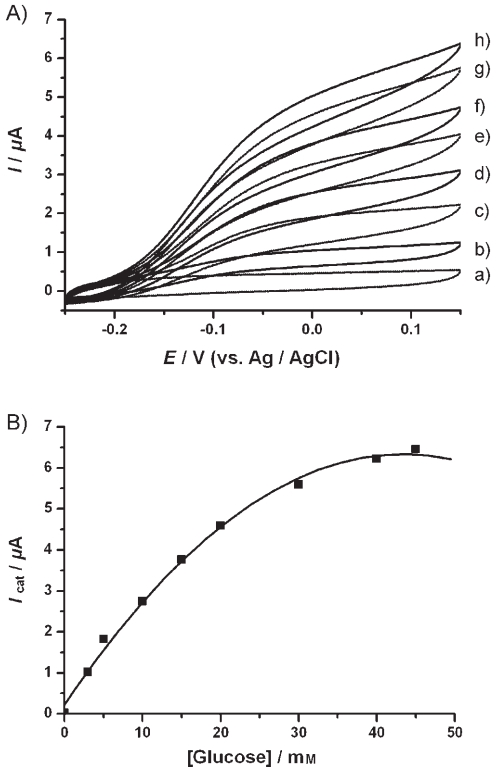

Figure 2. A) Cyclic voltammograms that correspond to the integrated GDH associated with $NADP^+$–**2**–**1**-functionalized SWCNT electrode in the presence of different concentrations of glucose: a) 0, b) 3, c) 5, d) 10, e) 15, f) 20, g) 30, h) 40 mM. Data were recorded in 0.10 M phosphate buffer (pH 7.0) under Ar at room temperature at a potential scan rate of 5 mV s^{-1}. B) Calibration curve that corresponds to the electrocatalytic currents measured at $E = 0.1$ V at variable concentrations of glucose.

Exclusion of either GDH or $NADP^+$, or by directly linking $NADP^+$ to the SWCNT through **2** in the absence of **1**, did not yield any electrocatalytic oxidation of glucose. These control experiments imply that all of the components are essential to activate the bioelectrocatalyzed oxidation of glucose, and that the electrical contact of GDH is the result of the **1**-mediated oxidation of NADPH generated by the GDH-catalyzed oxidation of glucose.

Similar results were observed with AlcDH. The electrically contacted enzyme electrode was assembled according to Scheme 1B. Figure 3A shows the cyclic voltammograms that correspond to the analysis of different concentrations of ethanol by the SWCNT-modified electrode. As the concentration of ethanol is increased, the electrocatalytic anodic currents are higher. The calibration curve is shown in Figure 3B. Also, the control experiments in which the bioelectrocatalytic oxidation of ethanol was examined by the electrode functionalized with the NAD^+–**1** conjugate-modified SWCNT in the presence of diffusional AlcDH revealed that **1**, as well as NAD^+, are essential to stimulate the bioelectrocatalyzed oxidation of ethanol. These results demonstrated that the electrical contact of AlcDH with the electrode is a result of **1**-mediated oxidation of NADH generated by the AlcDH-catalyzed oxidation of ethanol. In these systems, the onset potential of the electrocatalytic anodic currents are observed at the redox potential of the units of **1** functionalized with **2**, which implies that these sites mediate the bioelectrocatalyzed oxidation of alcohol. It should be noted that the integrated electrodes that consist of GDH–$NAD(P)^+$ and AlcDH–NAD^+ had good stability. Under continuous operation for 12 h, the electrochemical responses of the electrodes decreased by less than 5%. Furthermore, it should be noted that the specific structures that include **1** as a mediator are essential for electrical communication with the redox enzymes and the electrodes. Mediator **1** does not associate with other materials, for example, GC, and hence, the specific structures cannot be constructed on such materials. Also, the currents observed in the present study are substantially higher than those observed for mediated NAD^+-dependent enzymes in other porous matrices.[21]

As mentioned earlier, the $NADP^+$ cofactor can only form one type of complex with **2**, whereas the NAD^+ cofactor units can link to **2** in two different configurations. These configurations may differ in their efficiencies in electrical contact with the bound enzyme, and thus, it is important to elucidate the possible existence of the two configurations and their structure–catalytic function relationships. Chronoamperometry provides a very sensitive method to identify isomeric redox structures associated with electrodes or similar redox species linked to electrodes at different distan-

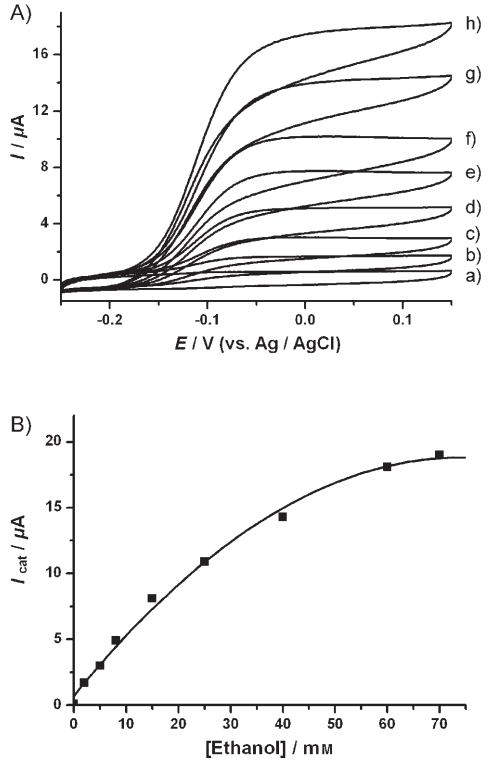

Figure 3. A) Cyclic voltammograms that correspond to the integrated AlcDH associated with a NAD^+–**2**–**1**-functionalized SWCNT electrode in the presence of different concentrations of ethanol: a) 0, b) 2, c) 5, d) 8, e) 15, f) 25, g) 40, h) 60 mM. Data were recorded in 0.10 M phosphate buffer (pH 7.0) under Ar at room temperature at a potential scan rate of 5 mV s^{-1}. B) Calibration curve that corresponds to the electrocatalytic currents measured at $E=0$ V at variable concentrations of ethanol.

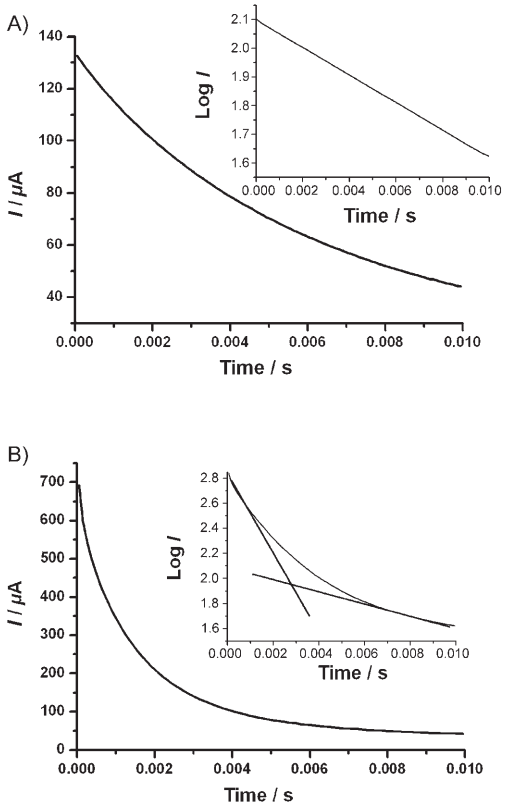

Figure 4. A) Chronoamperometric current transient that corresponds to the pulsed bioelectrocatalytic oxidation of glucose by integrated GDH associated with $NADP^+$–**2**–**1**–SWCNT-functionalized GC electrode in the presence of glucose (40 mM). The transient current was recorded by applying a potential step from $E_{initial}=-0.3$ V to $E_{final}=0.15$ V. Inset: The time-dependent current transient in a semilogarithmic plot according to Equation 1. B) Chronoamperometric current transient that corresponds to the pulsed bioelectrocatalytic oxidation of ethanol by integrated AlcDH associated with NAD^+–**2**–**1**–SWCNT-functionalized GC electrode in the presence of ethanol (60 mM). The current transient was recorded by applying a potential step from $E_{initial}=-0.3$ V to $E_{final}=0.15$ V. Inset: The time-dependent current transient in a semilogarithmic plot according to Equation (1). Data were recorded in a 0.10 M phosphate buffer (pH 7.0) under Ar at room temperature.

ces.[22] It was shown that the transient current upon the oxidation (or reduction) of an identical redox species associated to an electrode in different structural positions is given by Equation (1), in which k_{et}^1 and k_{et}^2 are the electron-transfer rate constants to (or from) two different structurally positioned redox species linked to the electrode, and Q_1 and Q_2 are the charges associated with the reduction (or oxidation) of the respective redox species (the respective surface coverages).

$$I(t) = k_{et}^1 Q_1 \exp(-k_{et}^1 t) + k_{et}^2 Q_2 \exp(-k_{et}^2 t) \quad (1)$$

Indeed, this method was successfully applied to characterize composite redox-active monolayers[22] and to identify dynamic transformations of redox-active units linked to the electrode.[23] In the present study, we have successfully applied the method to probe the binding modes of $NADP^+$ and NAD^+ to **2** in the two integrated enzyme electrodes. Figure 4A shows the chronoamperometric transient observed upon the application of an oxidative potential step on the GDH–$NADP^+$ integrated enzyme electrode. The transient follows single exponential kinetics, $k_{et}=(160\pm 20)$ s^{-1} (Figure 4A, inset). From the derived pre-exponential factor and knowing the electron-transfer rate constant, the surface coverage of the active, electrically contacted GDH–$NADP^+$ complex was estimated to be 6.01×10^{-10} moles cm^{-2}. Figure 4B depicts the chronoamperometric transient that corresponds to the AlcDH–NAD^+ integrated electrode upon the application of the oxidative potential step. Clearly, the current transient indicates biexponential kinetics. The inset of Figure 4B shows that one bioelectrocatalytic process proceeds with fast kinetics, $k_{et}^1=(870\pm 30)$ s^{-1}, and a second bioelectrocatalytic reaction occurs at a substantially slower rate, $k_{et}^2=(150\pm 20)$ s^{-1}. The two routes for forming the electrical contact in the NAD^+-dependent biocatalyst are attributed to two different binding modes of NAD^+ to **2**. The slow electron-transfer process (similar to that observed by the $NADP^+$ cofactor) is attributed to the biocatalyzed oxidation of ethanol by the NAD^+ cofactor linked to **2** through the ribose unit adjacent to the nicotin-

amide site. The fast electron-transfer process is attributed to the NAD^+ cofactor units linked to **2** by the ribose unit adjacent to the adenine group.

The success in constructing integrated, electrically contacted $NAD(P)^+$-dependent enzyme–SWCNT-based electrodes suggests that, aside from the use of the functionalized electrodes for the amperometric detection of their respective substrates, the electrodes could be used as biocatalytic anodes for biofuel cells. Towards this end, we have used bilirubin oxidase (BOD) in electrical contact with a SWCNT-based electrode as the cathode material. This electrode was previously reported to be a biocatalytic cathode for the four-electron reduction of O_2 to H_2O.[24] BOD includes four-copper atoms that participate in the electron transfer and activation of O_2 in the reduction process. [25] BOD was adsorbed onto the SWCNTs and crosslinked by glutaric dialdehyde. Figure 5A shows the cyclic voltammograms of the BOD-modified SWCNT electrode under argon (curve a) and under O_2 (curve b). In the presence of O_2 a cathodic current is observed with an onset potential that corresponds to 0.50 V versus Ag/AgCl. Control experiments revealed that no cathodic current was observed with SWCNT-modified electrodes that were not associated to BOD. Thus, BOD associated with the SWCNTs acts as the biocatalyst that is in direct electrical contact with the electrode through the SWCNTs, and it catalyzes the reduction of O_2 to H_2O. The direct electrical contact of the copper sites of BOD with the SWCNTs is further supported by the cathodic waves observed for the copper centers of the protein bound to the SWCNTs. Figure 5B and C show the differential pulse voltammograms of bare SWCNTs linked to the electrode and of the crosslinked BOD associated with the SWCNTs that were deposited on the electrodes, respectively. The BOD-modified electrode has two waves at 0.19 and 0.42 V versus Ag/AgCl that are attributed to the copper sites in the biocatalyst. These values are in good agreement with the reported values of 390 and 670 mV versus NHE.[26] We note, however, that adsorption of BOD onto the GC electrode did not lead to any voltammetric response of the copper centers in the enzyme, and the resulting electrode did not reveal any bioelectrocatalytic function towards the reduction of O_2. Thus, the adsorption of BOD onto the SWCNTs is essential to activate the enzyme towards the electrocatalytic reduction of O_2.

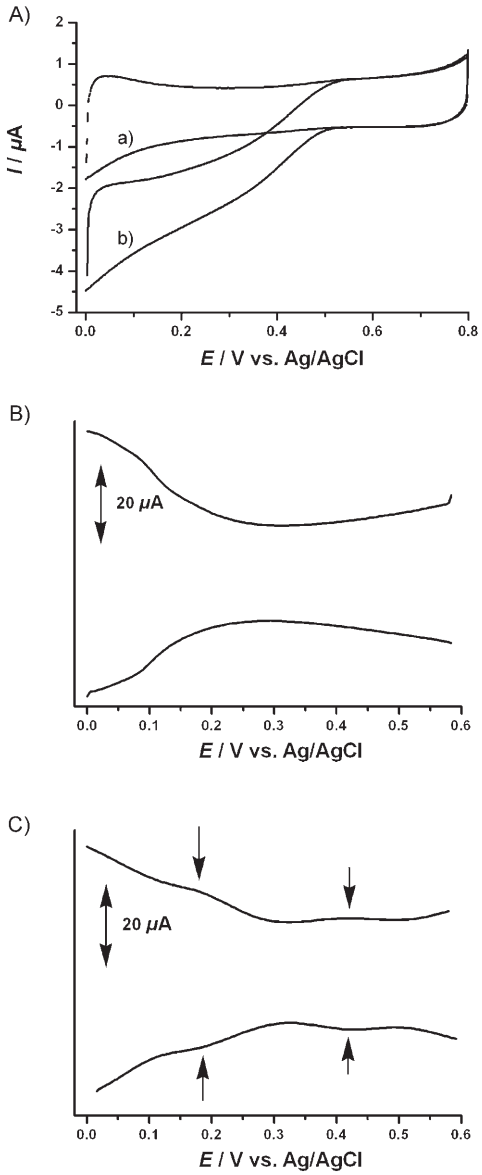

Figure 5. A) Cyclic voltammograms that correspond to the BOD–SWCNT-modified GC electrode a) under Ar and b) under O_2. Data recorded in 0.10 M phosphate buffer (pH 7.0) at a scan rate of 10 mVs^{-1}. B) and C) Differential potential voltammograms that correspond to bare SWCNTs and BOD–SWCNT-modified GC electrodes under Ar, respectively. Data recorded in 0.10 M phosphate buffer, pH 7.0.

The difference between the anode electrodes, GDH–$NADP^+$–**1**–SWCNT or AlcDH–NAD^+–**1**–SWCNT, and the BOD–SWCNT electrodes is approximately $\Delta E = 650$ mV. The operation of biofuel cells that consist of the glucose/O_2 or ethanol/O_2 anode and the BOD/O_2 cathode was examined (Scheme 2). The current densities (○ in Figure 6A) and electrical power densities (■ in Figure 6A) at different external resistances for the GDH/glucose|BOD/O_2 biofuel cell were determined. Similarly, the current densities (○ in Figure 6B) and electrical power densities (■ in Figure 6B) of the AlcDH/alcohol|BOD/O_2 biofuel cell were also determined. The maximum power output corresponds to 48 μW cm^{-2}. Although the power outputs of the biofuel cells are low, the results indicate the successful construction of the SWCNT-based biofuel cells that use $NAD(P)^+$-dependent enzymes as the biomaterial for the preparation of the biocatalytic anodes. The power output of the two cells is almost identical, which is not surprising in view of the fact that the power output of the two cells is controlled and limited by the biocatalytic BOD-stimulated reduction of O_2. The low electrocatalytic current values observed for the O_2 reduction process by the BOD–SWCNT electrode (Figure 5A) suggest that the biocatalyzed reduction of O_2 is inefficient and it limits the operation of the two biofuel cells. It should be noted that the power output from the present

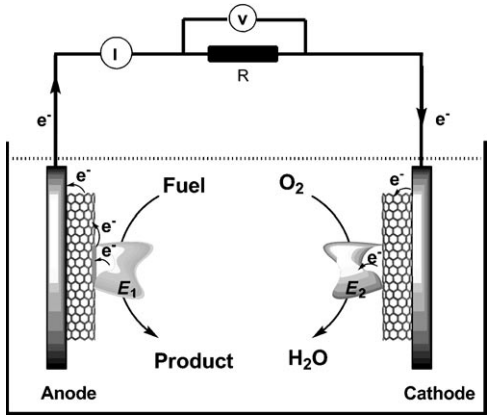

Scheme 2. Scheme for the biofuel cell that consists of bioelectrocatalytic electrodes composed of electrically contacted enzyme–SWCNTs.

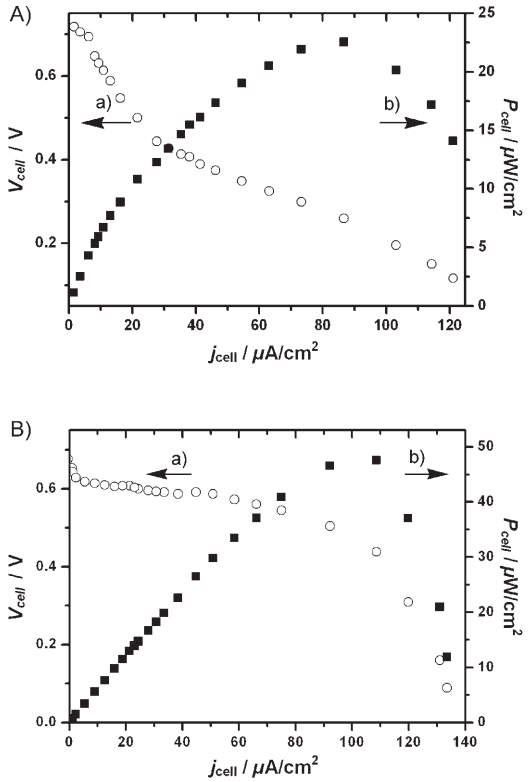

Figure 6. A) Cell polarization curve (a) and the dependence of the cell power (b) on the current of the GDH/glucose|BOD/O_2 biofuel cell. The supporting electrolyte was 0.10 M phosphate buffer (pH 7.0) that included glucose (40 mM) and saturated with O_2. B) Cell polarization curve (a) and the dependence of the cell power (b) on the current of the AlcDH/ethanol|BOD/O_2 biofuel cell. The supporting electrolyte was 0.10 M phosphate buffer (pH 7.0) that included O_2-saturated ethanol (60 mM).

biofuel cells is still substantially lower than the values observed with redox proteins in electrical contact in polymer hydrogels.[1b] However, we employ a substantially thinner SWCNT layer than in the polymer matrices. Thus, one might anticipate that by the layer-by-layer deposition of SWCNTs and by improving the turnover of the O_2 reducing electrode, the power outputs of our systems could be significantly improved.

Conclusion

The present study has demonstrated the successful assembly of integrated, electrically contacted NAD(P)$^+$-dependent enzyme–SWCNT electrodes. The resulting electrodes were used for the amperometric analysis of glucose or ethanol. The GDH–SWCNT and AlcDH–SWCNT electrodes were also used as the anodes in the construction of SWCNT-based integrated biofuel cells. Towards this goal, a BOD-functionalized SWCNT-based electrode was used as the cathode. The electrical power outputs of the resulting biofuel cells are rather low, but they demonstrate the successful construction of SWCNT-based biofuel cells based on NAD(P)$^+$-dependent enzymes. Further attempts to enhance the power output of the biofuel cells by improving the BOD cathode performance through the immobilization of BOD in redox polymers or the reconstitution of BOD (or laccase) on copper complexes associated with SWCNTs are underway in our laboratory.

Experimental Section

Chemicals: SWCNTs (with an average diameter of about 2 nm and a length of about 50 μm) were purchased from Nanoport (Shenzhen, China). The SWCNTs were purified by heating the as-received SWCNTs at reflux in 2.6 M HNO_3 for 10 h followed by precipitation and rinsing with water. AlcDH (E.C. 1.1.1.1, activity of 451 U mg^{-1}), GDH (E.C. 1.1.1.47, activity of 216 U mg^{-1}), and BOD (from *Myrothecium verrucaria*, E.C. 1.3.3.5, activity of 5 U mg^{-1} solid) were purchased from Sigma and used without further purification. NAD$^+$ and NADP$^+$ were purchased from Sigma and used without further purification. All other chemicals, which included **1**, **2**, 4-(2-hydroxyethyl)piperazine-1-ethanesulfonic acid sodium salt (HEPES), 1-ethyl-3-(3-dimethylaminopropyl)carbodiimide (EDC), glutaric dialdehyde, β-D-(+)-glucose, and ethanol were purchased from Sigma and Aldrich and used as supplied. Ultrapure water from a Nanopure (Barnstead) source was used throughout this work.

Modification of electrodes: GC electrodes (3 mm diameter) were purchased from Bioanalytical Systems (West Lafayette, IN). The electrodes were first polished with emery paper (# 2000), 0.3 and 0.05 μm alumina slurry on a polishing cloth, then cleaned in a sonication bath for 10 min, and finally thoroughly rinsed with distilled water. SWCNTs were dispersed in DMF (1 mg mL^{-1}) to yield a stable suspension. The dispersion (2 μL) was deposited onto the GC electrodes to generate the SWCNT-modified GC electrode. The resulting air-dried SWCNT-modified electrodes were immersed into an aqueous solution of **1** (0.10 mM) for 2 h. The electrodes were thoroughly rinsed with water and the **1**-functionalized SWCNT-modified GC electrodes were then treated with a solution of **2** (1 mM) in 0.1 M HEPES buffer (pH 7.5) in the presence of EDC (5 mM) for 2 h. The resulting electrodes were rinsed with water. The SWCNT-modified GC electrodes functionalized with **1** and covalently bound **2** were used for further functionalization with NAD$^+$ or NADP$^+$. The functionalized electrodes were treated with the respective cofactor solution (1 mM) in 0.10 M phosphate buffer (pH 7.0) for 2 h and then washed with buffer. This treatment resulted in the formation of SWCNT-modified GC electrodes functionalized with redox-relay **1** and the respective cofactor unit (NAD$^+$ or NADP$^+$) covalently bound to the SWCNT sur-

face through **2**. The NAD^+–**1**- or $NADP^+$–**1**-functionalized SWCNT-modified GC electrodes were coated with stock solutions (5 μL) of AlcDH (5 mg mL^{-1}) or GDH (2 μL), respectively, in 0.10 M phosphate buffer (pH 7.0) and then treated with glutaric dialdehyde (10% v/v) in 0.10 M phosphate buffer (pH 7.0) for 2 h at 4 °C. The resulting SWCNT-modified GC electrodes were washed with phosphate buffer to yield the crosslinked AlcDH–NAD^+ integrated electrodes for the biocatalytic oxidation of ethanol, and the crosslinked GDH–$NADP^+$ integrated electrodes for the biocatalytic oxidation of glucose. The biocathode for the biofuel cells was prepared by depositing and crosslinking solutions of BOD/BSA (0.3 U, 1:1 v/v) onto SWCNT-modified GC electrodes by using an aqueous solution of glutaric dialdehyde (40 mM, 1 μL). The electrodes were dried at 4 °C in a refrigerator and used as the biocathode for the biofuel cells.

Biofuel cells and electrochemical measurements: A conventional three-electrode cell, which consisted of the enzyme-integrated, SWCNT-modified GC working electrode, a GC auxiliary electrode isolated by a glass frit, and a KCl saturated Ag/AgCl electrode connected to the working volume with a Luggin capillary, was used for the electrochemical measurements. All potentials are reported with respect to Ag/AgCl. Argon bubbling was used to remove oxygen from the solutions in the electrochemical cell unless otherwise stated. The cell was placed in a grounded Faraday cage. Cyclic voltammetry and chronoamperometry were performed by using an Autolab electrochemical system (ECO Chemie, the Netherlands). Differential pulse voltammograms were recorded in the potential range of 0 to 0.6 V with a step potential of 0.01 V and an amplitude potential of 0.05 V. For assembling the biofuel cells, the enzyme-integrated, SWCNT-modified GC AlcDH or GDH anode and the BOD cathode were placed into a 10 mL cell filled with 0.1 M phosphate buffer (pH 7.0) as an electrolyte in the presence of ethanol (60 mM) or glucose (40 mM) as fuels and O_2 as the oxidizer. Current–voltage polarization curves were measured on a variable external resistance by using an electrometer (Keithley 617). All electrochemical measurements were performed at ambient temperatures ((22 ± 2) °C).

Acknowledgements

Parts of the project are supported by the EdRox Marie Curie Research Training Network and BIOMEDNANO EC Projects.

[1] a) A. Heller, *Acc. Chem. Res.* **1990**, *23*, 128–134; b) A. Heller, *Phys. Chem. Chem. Phys.* **2004**, *6*, 209–216.

[2] a) I. Willner, E. Katz, B. Willner, *Electroanalysis* **1997**, *9*, 965–977; b) A. Heller, *J. Phys. Chem.* **1992**, *96*, 3579–3587; c) I. Willner, *Science* **2002**, *298*, 2407–2408.

[3] a) W. T. J. Schuhmann, T. J. Ohara, H.-L. Schmidt, A. Heller, *J. Am. Chem. Soc.* **1991**, *113*, 1394–1397; b) I. Willner, A. Riklin, B. Shoham, D. Rivenzon, E. Katz, *Adv. Mater.* **1993**, *5*, 912–915.

[4] a) N. Mano, V. Soukharev, A. Heller, *J. Phys. Chem. B* **2006**, *110*, 11180–11187; b) N . Mano, F. Mao, A. Heller, *J. Electroanal. Chem.* **2005**, *574*, 347–357; c) F. Mao, N. Mano, A. Heller, *J. Am. Chem. Soc.* **2003**, *125*, 4951–4957; d) A. Heller, *Curr. Opin. Chem. Biol.* **2006**, *10*, 664–672.

[5] B. Willner, E. Katz, I. Willner, *Curr. Opin. Biotechnol.* **2006**, *17*, 589–596.

[6] a) I. Willner, V. Heleg-Shabtai, R. Blonder, E. Katz, G. Tao, A. F. Bückmann, A. Heller, *J. Am. Chem. Soc.* **1996**, *118*, 10321–10322; b) E. Katz, L. Sheeney-Ichia, I. Willner, *Angew. Chem.* **2004**, *116*, 3354–3362; *Angew. Chem. Int. Ed.* **2004**, *43*, 3292–3300.

[7] O. A. Raitman, E. Katz, A. F. Bückmann, I. Willner, *J. Am. Chem. Soc.* **2002**, *124*, 6487–6496.

[8] a) Y. Xiao, F. Patolsky, E. Katz, J. F. Hainfeld, I. Willner, *Science* **2003**, *299*, 1877–1881; b) M. Zayats, E. Katz, R. Baron, I. Willner, *J. Am. Chem. Soc.* **2005**, *127*, 12400–12406.

[9] F. Patolsky, Y. Weizmann, I. Willner, *Angew. Chem. Int. Ed.* **2004**, *43*, 2113–2117.

[10] a) S. C. Barton, J. Gallaway, P. Atanassov, *Chem. Rev.* **2004**, *104*, 4867–4886; b) R. A. Bullen, T. C. Arnot, J. B. Lakeman, F. C. Walsh, *Biosens. Bioelectron.* **2006**, *21*, 2015–2045.

[11] I. Willner, G. Arad, E. Katz, *Bioelectrochem. Bioenerg.* **1998**, *44*, 209–214.

[12] E. Katz, I. Willner, A. B. Kotlyar, *J. Electroanal. Chem.* **1999**, *479*, 64–68.

[13] a) N. Mano, A. Heller, *J. Am. Chem. Soc.* **2005**, *127*, 11574–11575; b) V. Soukharev, N. Mano, A. Heller, *J. Am. Chem. Soc.* **2004**, *126*, 8368–8369.

[14] E. Katz, I. Willner, *J. Am. Chem. Soc.* **2003**, *125*, 6803–6813.

[15] E. Katz, O. Lioubashevski, I. Willner, *J. Am. Chem. Soc.* **2005**, *127*, 3979–3988.

[16] a) T. Chen, S. C. Barton, G. Binyamin, Z. Q. Gao, Y. C. Zhang, H. H. Kim, A. Heller, *J. Am. Chem. Soc.* **2001**, *123*, 8630–8631; b) N. Mano, F. Mao, A. Heller, *J. Am. Chem. Soc.* **2003**, *125*, 6588–6594.

[17] I. Katakis, E. Dominguez, *Mikrochim. Acta* **1997**, *126*, 11–32.

[18] M. Zayats, E. Katz, I. Willner, *J. Am. Chem. Soc.* **2002**, *124*, 14724–14735.

[19] a) M. G. Zhang, W. Gorski, *Anal. Chem.* **2005**, *77*, 3960–3965; b) N. S. Lawrence, J. Wang, *Electrochem. Commun.* **2006**, *8*, 71–76.

[20] a) Y. M. Yan, W. Zheng, L. Su , L. Q. Mao, *Adv. Mater.* **2006**, *18*, 2639–2643; b) Y. M. Yan, M. N. Zhang, K. P. Gong, L. Su, Z. X. Guo, L. Q. Mao, *Chem. Mater.* **2005**, *17*, 3457–3463; c) I. Willner, A. Riklin, *Anal. Chem.* **1994**, *66*, 1535–1539; d) A. Malinauskas, T. Ruzgas, L. Gorton, *J. Electroanal. Chem.* **2000**, *484*, 55–63; e) F. D. Munteanu, N. Mano, A. Kuhn, L. Gorton, *Bioelectrochemistry* **2002**, *56*, 67–72; f) F. D. Munteanu, N. Mano, A. Kuhn, L. Gorton, *J. Electroanal. Chem.* **2004**, *564*, 167–178; g) A. A. Karyakin, E. E. Karyakina, H. L. Schmidt, *Electroanalysis* **1999**, *11*, 149–155.

[21] S. Ben-Ali, D. A. Cook, P. N. Bartlett, A. Kuhn, *J. Electroanal. Chem.* **2005**, *579*, 181–187.

[22] E. Katz, I. Willner, *Langmuir*, **1997**, *13*, 3364–3373.

[23] I. Willner, V. Heleg-Shabtai, E. Katz, H. K. Rau, W. Haehnel, *J. Am. Chem. Soc.* **1999**, *121*, 6455–6468.

[24] F. Gao, Y. M. Yan, L. Su, L. Wang, L. Q. Mao, *Electrochem. Commun.* **2007**, *9*, 989–996.

[25] a) S. Shleev, J. Tkac, A. Christenson, T. Ruzgas, A. I. Yaropolov, J. W. Whittaker, L. Gorton, *Biosens. Bioelectron.* **2005**, *20*, 2517–2554; b) S. Shleev, A. E. Kasmi, T. Ruzgas, L. Gorton, *Electrochem. Commun.* **2004**, *6*, 934–939.

[26] A. Christenson, S. Shleev, N. Mano, A. Heller, L. Gorton, *Biochim. Biophys. Acta Bioenerg.* **2006**, *1757*, 1634–1641.

Received: May 27, 2007
Published online: October 15, 2007

